



High Electrocatalytic Activity of Platinum Nanoparticles on SnO₂ Nanowire-Based Electrodes

Madhu Sudan Saha,^{a,*} Ruying Li,^a Mei Cai,^b and Xueliang Sun^{a,*z}

^aDepartment of Mechanical and Materials Engineering, The University of Western Ontario, London, Ontario N6A 5B9, Canada

^bGeneral Motors Research and Development Center, Warren, Michigan 48090-9055, USA

The composite electrodes were prepared by electrochemical deposition of platinum (Pt) nanoparticles onto the surface of tin oxide (SnO₂) nanowires directly grown on the carbon fibers of a carbon paper. This is the first report of an electrode design using Pt catalyst supported on a SnO₂ nanowire-based electrode. In the comparison to a standard Pt/C electrode, the nanowire-based electrode exhibited higher electrocatalytic activity both for oxygen reduction reaction and methanol oxidation reaction. The results imply that nanowire-based composite electrodes are excellent potential candidates for application in proton exchange membrane and direct methanol fuel cells.

© 2007 The Electrochemical Society. [DOI: 10.1149/1.2745632] All rights reserved.

Manuscript submitted March 13, 2007; revised manuscript received May 7, 2007. Available electronically June 11, 2007.

Proton exchange membrane fuel cells (PEMFCs) have been intensively investigated in recent years as an alternative power source for stationary and mobile applications. The high power density of PEMFC stacks and low emissions provide potential applications in automotive applications, but barriers to widespread implementation remain due to hydrogen fuel infrastructure, durability, and cost issues.^{1,2} Currently, platinum (Pt) supported on high-surface-area carbon materials is the only feasible electrocatalyst system for the electrochemical reduction of oxygen in acidic media. The catalytic activities highly depend on the size and dispersion of Pt particles onto the support as well as the particle interactions with the support substrates.^{3,4} Until now, carbon black (Vulcan XC-72R) has been the most widely used fuel cell catalyst support due to its good electronic conductivity, high surface area, good electrochemical performance, and stability in acidic environment.⁵ However, recent investigations into the deterioration of overall cell performance have revealed that a considerable part of the performance loss is due to the degradation of the electrocatalyst system.⁶ The degradation mechanisms proposed include Pt sintering,⁷ Pt dissolution,⁸ and carbon corrosion of the support substrate.⁹ Also, during the preparation of the electrocatalyst, the Pt nanoparticles can be trapped in deep cracks of carbon black, which reduces the number of three-phase boundary reactive sites, thus reducing the Pt utilization.¹⁰ It has been suggested that because the catalyst support plays such an important role in cell performance, the ideal catalyst support would be both gas and water permeable and conduct both protons and electrons.¹¹ Therefore, to improve catalytic activities and durability of the electrocatalysts, a stable support with a three-dimensional (3D) structure and a high surface area is highly desirable.^{12,13}

Recently, carbon nanotubes (CNTs) and nanofibers (CNFs) have attracted great attention as promising catalyst supports because of their unique properties, such as high surface area, good electronic conductivity, strong mechanical properties, and chemical stability.^{14,15} A number of research groups have demonstrated the advantages of using CNTs or CNFs as supports to better disperse Pt and its alloys for oxygen reduction and methanol oxidation reactions.¹⁶⁻¹⁸ In particular, the nanotube-based 3D electrode structure has shown very promising implications.^{12,19}

Compared to CNTs, nanowires (NWs) are a class of one-dimensional nanomaterials with a high aspect ratio. Unlike CNTs, NWs can be made of various compositions of materials and they have solid cores. NWs have demonstrated superior electrical, optical, mechanical, and thermal properties.²⁰⁻²² The broader choice of various crystalline materials and easier doping methods provide highly tunable properties (e.g., electrical) of NWs. Among various kinds of nanowires, metal oxide NWs have several unique advan-

tages as supports for dispersing noble metal nanoparticles such as Pt for practical applications. First, certain metal oxide materials such as SnO₂ show very high catalytic properties; the combination of this type of metal oxide materials with noble metal nanoparticles should certainly have enhanced catalyst activities toward methanol oxidation.^{23,24} Second, there is a very strong interaction between noble metal nanoparticles and metal oxide surface.⁴ Finally, NWs grown on carbon-paper fuel cell backings form a 3D structure that leads to a higher gas permeability. We expect that NW-based 3D structure will take full advantage of combined factors including increased utilization of the noble metal catalyst, improved metal-support interaction, and enhanced mass transport in the electrodes for fuel cell applications.

SnO₂ is a popular semiconducting material and has been extensively studied due to its potential applications in many technological areas such as chemical sensors²⁵ and electronic devices.²⁶ Recently, SnO₂ in the form of small particles have been used for PEMFCs and direct methanol fuel cells (DMFCs).²⁴ The uniqueness of the work reported here, compared to previous work reported in the literature, is to grow SnO₂ NWs directly on the carbon fibers of carbon paper by a thermal evaporation method, followed by deposition of Pt nanoparticles onto SnO₂ NWs. Our process ensures that all the deposited Pt particles are in electrical contact with the external electrical circuit. The results from this study are a demonstration of SnO₂ NW-based composite electrodes consisting of Pt nanoparticles supported on SnO₂ NWs grown on carbon paper. The electrocatalytic activities of this composite electrode for oxygen reduction and for the methanol oxidation reaction are also reported here.

Experimental

SnO₂ NWs were grown directly on the fibers of a carbon paper (E-TEK, a division of De Nora North America, Somerset, NJ) by a thermal evaporation method. In a typical experiment, an alumina boat (7.5 × 1.2 cm) loaded with pure commercial Sn powders (2 g, 325 mesh, 99.8%) was placed in the middle of a quartz tube (1.8 cm inner diameter and 75 cm length) and inserted into a horizontal tube furnace. A small piece of carbon paper was placed beside the metal powder. The reaction chamber was heated to 800–900°C rapidly (in about 15 min) from room temperature with an argon (Ar) flow rate of 200 sccm. Subsequently, the furnace was kept at 800°C for 2 h and then cooled to room temperature. After the reaction, a dense, white wool-like product was observed on the surface of the carbon substrate. During the heating, the Sn vapor generated from the Sn powder combined with oxygen, which comes from the residue O₂ in the reaction chamber or from the Ar gas, to form SnO₂ NWs. This product was analytically confirmed as SnO₂ NWs grown on carbon fibers.

The electrochemical measurements were carried out by using an Autolab potentiostat/galvanostat (model PGSTAT-30, Ecochemie,

* Electrochemical Society Active Member.
 z E-mail: xsun@eng.uwo.ca

Brinkman Instruments). A standard three-electrode cell with two-compartment configuration was used. A platinum foil was used as the counter electrode. A saturated calomel electrode (SCE) was used as the reference electrode, and all potentials reported in this paper are vs SCE. The purified Ar and oxygen gases used for measurements were purchased from Praxair Canada Inc.

Before the process of Pt nanoparticle deposition, the SnO_2 NWs grown on carbon paper (SnO_2 NWs/carbon paper) were pretreated chemically with 5.0 M HNO_3 aqueous solution for 5 h. In order to increase the electrochemical activity of the SnO_2 NWs in water solution, the SnO_2 NWs/carbon paper electrode was placed in 0.1 M H_2SO_4 aqueous solution and repeatedly cycled through the potential range of -0.15 to $+1.3$ V vs SCE with a scan rate of 50 mV/s until steady curves were obtained.²⁷ This surface activation step produces oxide functional groups such as hydroxyl ($-\text{OH}$), carboxyl ($-\text{COOH}$), and carbonyl ($-\text{C}=\text{O}$) on the surface of the SnO_2 NWs.^{27,28}

The deposition of Pt nanoparticles onto the SnO_2 NW/carbon paper (Pt/ SnO_2 NW/carbon paper) was accomplished electrochemically with a similar procedure employed by others.²⁹ Octahedral complexes of Pt(IV) were formed on the surface of SnO_2 NWs placed in a solution of 3 mM K_2PtCl_4 and 0.1 M K_2SO_4 solutions by application of cyclic voltammetry (CV) under conditions of a potential range from $+0.34$ to $+1.34$ V at a scan rate of 5 mV/s. The surface complexes on the SnO_2 NWs were then converted to Pt nanoparticles by CV from $+1.64$ to -0.21 V in 0.1 M H_2SO_4 solution. The Pt/ SnO_2 NW/carbon paper composite electrode was cleaned with deionized water following the deposition and then evaluated for electrochemical properties. The Pt loading in the Pt/ SnO_2 NW/carbon paper composite was determined to be 0.12 mg/cm² by the "burning method"³⁰ (the total amount of Pt divided by the geometric surface area of the composite electrode).

For comparison purposes, a conventional electrode made with commercially available 30 wt % Pt/C from E-TEK, USA, was also evaluated. This electrode was prepared with a procedure similar to the one described by Gojković et al.³¹ Typically, 5 mg catalyst was sonically mixed with 1 mL 5 wt % Nafion solution (Ion Power, Inc.) to make a suspension. The catalyst films were prepared by dispersing 5 μL of the resultant suspension on a glassy carbon (GC, diameter: 3 mm) electrode to achieve a total Pt loading of 0.1 mg/cm² on the GC electrode. The catalyst films were dried in air at room temperature. The currents were normalized on the basis of Pt loading.

The morphologies of the electrode made with Pt nanoparticles deposited onto SnO_2 NW/carbon paper were examined using a scanning electron microscope (SEM) (Hitachi S-2600 N) and transmission electron microscopy (TEM) (Philips CM10).

Results and Discussion

Figure 1 shows the SEM and TEM images of the SnO_2 NWs grown on a commercially available carbon paper backing used in fuel cell applications. The carbon paper is made of small carbon fibers with a diameter between 5 and 10 μm (inset in Fig. 1a). As shown in Fig. 1a, a thin layer of high-density SnO_2 NWs completely covers the surface of the carbon fibers in the carbon paper. The length of the SnO_2 NWs is in the range of 20–30 μm . Further TEM examination shows that the NWs have a straight-line morphology with a diameter of about 20 nm (Fig. 1b). Figure 1c presents the TEM image of the Pt nanoparticles electrochemically deposited on the SnO_2 NWs. Pt nanoparticles with a size of 4–6 nm can be observed clearly on the surface of NWs. The successful deposition of Pt nanoparticles indicates a good electrical contact between the SnO_2 NWs and the carbon fibers.

Figure 2 shows the CVs of the $\text{Fe}(\text{CN})_6^{3-/4-}$ complex on a bare carbon paper and on SnO_2 NW/carbon paper composite electrodes. A much higher redox current and a larger surface area were obtained

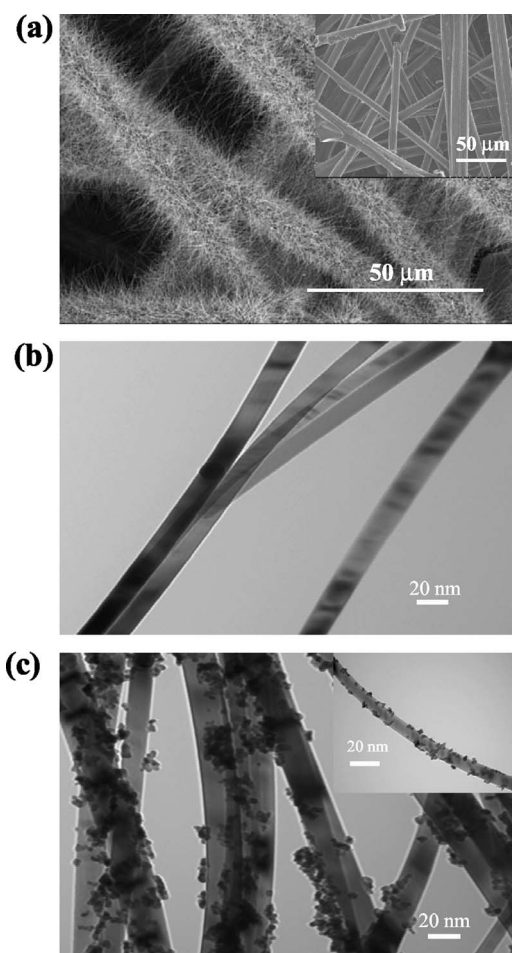


Figure 1. SEM and TEM micrographs of SnO_2 NWs grown on carbon fibers of carbon paper by thermal evaporation method. (a) SEM image showing full coverage of SnO_2 NWs on fibers of carbon paper. (Inset) Fibers of bare carbon paper. (b) TEM image showing individual SnO_2 NWs. (c) TEM images showing Pt nanoparticles electrochemically deposited onto SnO_2 NWs. (Inset) Pt nanoparticles deposited onto a single SnO_2 NW.

on SnO_2 NW/carbon paper composite electrode, strongly suggesting that the NWs are electrically connected to the carbon fibers of the fuel cell backing.

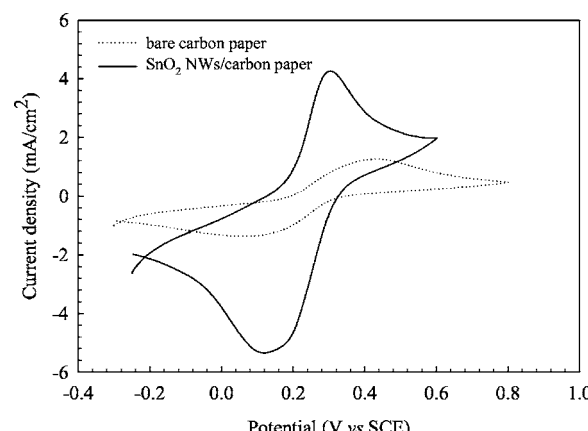


Figure 2. CVs in a $\text{K}_3\text{Fe}(\text{CN})_6$ aqueous solution (5 mM $\text{K}_3\text{Fe}(\text{CN})_6$ + 0.5 M K_2SO_4) of bare carbon paper and SnO_2 NWs grown on carbon paper at a scan rate of 50 mV/s. Current densities calculated with the geometric surface area.

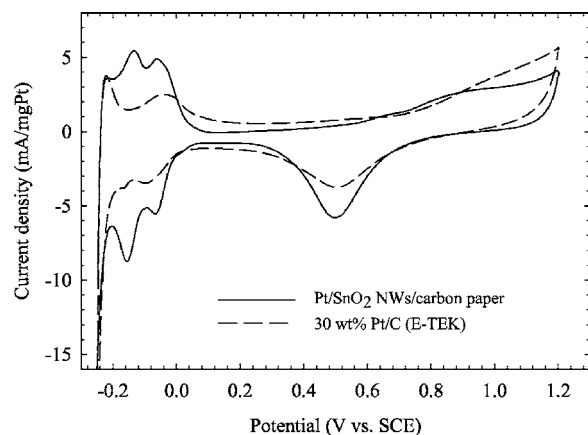


Figure 3. CVs of a Pt/SnO₂ NW/Carbon paper electrode with 0.12 mg/cm² Pt loading in Ar-saturated 0.5 M H₂SO₄ aqueous solution at room temperature. Potential scan rate 50 mV/s. A representative CV of a standard 30 wt % Pt/C electrode with 0.1 mg/cm² Pt loading is included for reference. The current normalized on the basis of Pt loading.

Figure 3 shows the CVs of SnO₂ NW/Carbon paper after electrodeposition of the Pt nanoparticles in Ar-saturated 0.5 M H₂SO₄ aqueous solution at room temperature. For comparison, the commercial Pt/C electrocatalyst from E-TEK (30 wt % Pt on carbon black) was also examined under the same conditions. The CVs were recorded between -0.25 and 1.2 V vs SCE at a scan rate of 50 mV/s. The voltammetric features of Pt/SnO₂ NW/Carbon paper composite electrode reveal the typical characteristics of Pt metal,³² with Pt oxide formation in the +0.63 to +1.2 V range, the reduction of Pt oxide at ca. +0.50 V, and the adsorption and deposition of hydrogen between -0.05 and -0.25 V. From the integration of the desorption peaks after excluding the double-layer charging effect, the total charges of hydrogen desorption (Q_H) on the Pt/SnO₂ NW/Carbon paper electrode and conventional Pt/C electrode were calculated at 13.8 and 7.1 mC/cm², respectively. The Pt areas were calculated electrochemically according to the following formula.¹³

$$A_{EL} = Q_H / [Q_{ref}(Pt \text{ loading})]$$

A_{EL} is expressed in cm²/mg, where Pt loading is in mg_{Pt}/cm² and $Q_{ref} = 0.21 \text{ mC/cm}^2$. This value corresponds to a surface density of $1.3 \times 10^{15} \text{ atom/cm}^2$, a generally accepted value for a polycrystalline Pt electrode³³

$$A_{EL} \text{ in } \text{m}^2/\text{g}_{\text{Pt}} = 0.1A_{EL} \text{ in } \text{cm}^2/\text{mg}_{\text{Pt}}$$

A value of $A_{EL} = 54.7 \text{ m}^2/\text{g}_{\text{Pt}}$ is obtained for the Pt/SnO₂ NW/Carbon paper electrode, while that for the commercial Pt/C electrode is $33.6 \text{ m}^2/\text{g}_{\text{Pt}}$. The specific electrochemical surface area of Pt/SnO₂ NW/Carbon paper electrode is 62% higher than the commercial Pt/C electrode. This result demonstrates a higher utilization of the Pt nanoparticles deposited onto SnO₂ NWs and a good electrical contact of Pt with the underlying SnO₂ NWs.

Figure 4a compares the CVs for oxygen reduction at a Pt/SnO₂ NW/Carbon paper electrode and a commercial Pt/C electrode. Compared with the SnO₂ NW/Carbon paper electrode (not shown), a significantly positive shift of the O₂ reduction potential and a concurrent increase in the O₂ reduction peak current were observed at the Pt/SnO₂ NW/Carbon paper electrode. The comparison of oxygen reduction with the standard Pt/C electrode was made at a Pt loading of 0.1 mg/cm². It can be seen that a 50 mV shift of the onset potential for oxygen reduction at the Pt/SnO₂ NW/Carbon paper electrode was observed as compared to Pt/C electrode. Lowering the onset potential by using the SnO₂ NW support is evidence for a stronger metal-support interaction between the Pt and SnO₂ NWs compared to Pt/C. It was previously reported that catalysts made with Pt nanoparticles deposited onto SnO₂ nanoparticles exhibited a

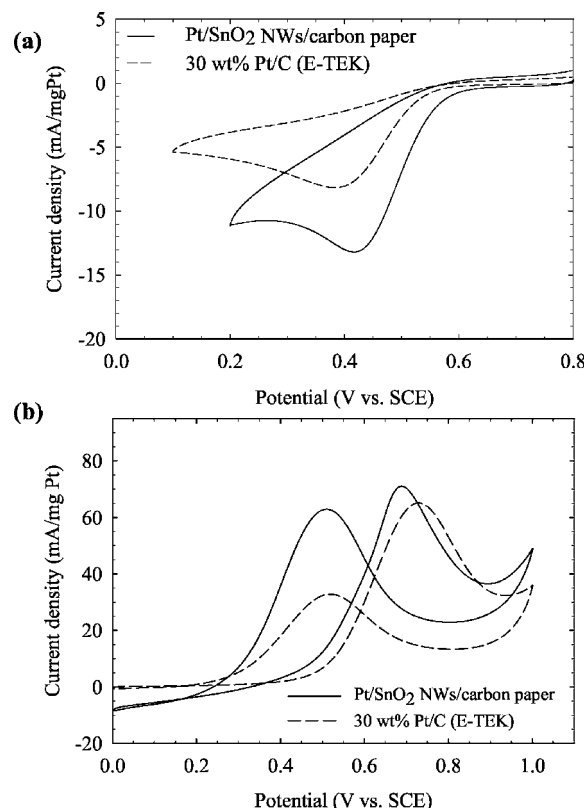


Figure 4. CVs for (a) oxygen reduction reaction in O₂-saturated 0.5 M H₂SO₄ and (b) methanol oxidation reaction in 1 M H₂SO₄ aqueous solution with 2 M MeOH at Pt/SnO₂ NW/Carbon paper with 0.12 mg/cm² Pt loading and standard 30 wt % Pt/C electrode with 0.1 mg/cm² Pt loading. Potential scan rate 50 mV/s. The current normalized on the basis of Pt loading.

strong chemical interaction between the Pt and SnO₂ surface, and this metal support interaction further improved the catalytic properties of the active metal through chemical effects.³⁴ The oxygen reduction peak current, normalized on the basis of Pt loading, is about 13.3 mA/mg_{Pt} for the Pt/SnO₂ NW/Carbon paper electrode, which is 1.6 times larger than that of Pt/C electrode (Fig. 4a). Further, the calculation of the specific activity (current normalized with Pt surface area) shows that the Pt/SnO₂ NW/Carbon paper electrode (0.025 mA/cm²_{Pt}) is slightly higher than the conventional Pt/C electrode (0.023 mA/cm²_{Pt}). These results imply that the Pt/SnO₂ NW/Carbon paper electrode shows good improvement in Pt utilization and slight improvement in oxygen reduction activity. Furthermore, the peak current varied linearly with the square root of the scan rate, indicating that oxygen reduction at the Pt/SnO₂ NW/Carbon paper electrode was a diffusion-controlled process.

The electrochemical performance of the Pt/SnO₂ NW/Carbon paper electrode for methanol oxidation was also examined and the corresponding results are shown in Fig. 4b. Before the deposition of Pt nanoparticles, no methanol oxidation was observed (not shown). After the Pt deposition, typical features of methanol oxidation were detected, which is in good agreement with literature.³⁵ Two oxidation peaks related to the oxidation of methanol and intermediates appeared at ca. 0.68 and 0.51 V, respectively. Compared with the Pt/C electrode, the oxidation peak current for the Pt/SnO₂ NW/Carbon paper electrode is about 71.5 mA/mg_{Pt}, which is higher than that of the Pt/C electrode (65.0 mA/mg_{Pt}), suggesting a higher utilization of Pt for methanol oxidation reaction. In terms of the specific activity defined above, no obvious difference can be observed for both electrodes.

This significant improvement in catalytic activities of the Pt/SnO₂ NW/Carbon paper composite electrode may be attributed to

the following: (*i*) the unique 3D structure and electronic properties of SnO₂ NWs, (*ii*) strong interaction between Pt catalyst particles and the SnO₂ NW surface, (*iii*) synergies resulting from the combined properties of Pt nanoparticles and SnO₂ NW supports, and (*iv*) low impurities of SnO₂ NWs compared to Vulcan carbon XC-72 which contains a significant amount of organosulfur impurities, which can poison the Pt metal.³⁶

One of the major concerns for the application of NWs to catalyst supports in PEMFCs and DMFCs is whether there is strong adhesion of these NWs to the carbon paper during actual fuel cell operation. To address this concern, we have carried out preliminary studies by immersing the SnO₂ NW/carbon paper composite electrode in 0.1 M H₂SO₄ solution over a period of 2 months at 50°C. SEM examinations after the test show that high-density NWs are maintained on the surface of carbon fibers, suggesting strong adhesion between SnO₂ NWs and the carbon paper. A more detailed study on the stabilities of SnO₂ NWs is currently in progress in our laboratory.

Conclusions

The composite electrodes of Pt/SnO₂ NW/carbon paper have been successfully synthesized for the first time. High electrocatalytic activities of the Pt/SnO₂ NW/carbon paper composite electrode for both oxygen reduction reaction and methanol oxidation reaction have been achieved in comparison with standard Pt/C electrode. The higher electrocatalytic activities are attributed to the enhanced properties achieved by combining Pt nanoparticles with the SnO₂ NW supports as well as the 3D composite electrode structure. Such a hierarchical electrode with the combined properties has potential applications for fuel cells. This approach also provides a route to fabricate electrodes based on depositing noble metal nanoparticles onto metal oxide NWs grown on the fuel cell backings.

Acknowledgments

This research was supported by General Motors of Canada, Natural Sciences and Engineering Research Council of Canada (NSERC), Canada Foundation for Innovation (CFI), Ontario Early Researcher Award (ERA), and the University of Western Ontario, Academic Development Fund (ADF) and the Start-up Fund.

The University of Western Ontario assisted in meeting the publication costs of this article.

References

- K. Lee, J. Zhang, H. Wang, and D. P. Wilkinson, *J. Appl. Electrochem.*, **36**, 507 (2006).
- H. A. Gasteiger, S. S. Kocha, B. Sompalli, and F. T. Wagner, *Appl. Catal., B*, **56**, 9 (2005).
- A. Gamez, D. Richard, P. Gallezot, F. Gloaguen, R. Faure, and R. Durand, *Electrochim. Acta*, **41**, 307 (1996).
- S. J. Tauster, S. C. Fung, R. T. K. Baker, and J. A. Horsley, *Science*, **211**, 1121 (1981).
- Q. Lu, B. Yang, L. Zhuang, and J. Lu, *J. Phys. Chem. B*, **109**, 1715 (2005).
- E. Gulzow, H. Sander, N. Wagner, M. Lorenz, A. Schneider, and M. Schulze, *Proceedings of the 2000 Fuel Cell Seminar*, p. 156 (2000).
- M. S. Wilson, H. G. Garzon, K. E. Sickafus, and S. Gottesfeld, *J. Electrochem. Soc.*, **140**, 2872 (1993).
- R. M. Darling and J. P. Myers, *J. Electrochem. Soc.*, **150**, A1523 (2003).
- L. M. Roen, C. H. Paik, and T. D. Jarvi, *Electrochem. Solid-State Lett.*, **7**, A19 (2004).
- S. D. Thompson, L. R. Jordan, and M. Forsyth, *Electrochim. Acta*, **46**, 1657 (2001).
- Z. Qi, Mark C. Lefebvre, and P. G. Pickup, *J. Electroanal. Chem.*, **459**, 9 (1998).
- C. Wang, M. Waje, X. Wang, J. M. Tang, R. C. Haddon, and Y. Yan, *Nano Lett.*, **4**, 345 (2004).
- D. Villers, S. H. Sun, A. M. Serventi, and J. P. Dodelet, *J. Phys. Chem. B*, **110**, 25916 (2006).
- P. M. Ajayan and O. Z. Zhou, *Top. Appl. Phys.*, **80**, 391 (2001).
- C. Pham-Huu, N. Keller, V. V. Roddatis, G. Mestl, R. Schloegl, and M. J. Ledoux, *Phys. Chem. Chem. Phys.*, **4**, 514 (2002).
- G. Che, B. B. Lakshmi, E. R. Fisher, and C. R. Martin, *Nature (London)*, **393**, 346 (1998).
- W. Li, C. Liang, W. Zhou, J. Qiu, Z. Zhou, G. Sun, and Q. Xin, *J. Phys. Chem. B*, **107**, 6292 (2003).
- N. Rajalakshmi, H. Ryu, M. M. Shajumon, and S. Ramaprabhu, *J. Power Sources*, **140**, 250 (2005).
- X. Sun, R. Li, D. Villers, J. P. Dodelet, and S. Desilets, *Chem. Phys. Lett.*, **379**, 99 (2003).
- Nanomaterials: Synthesis, Properties and Applications*, A. S. Edelstein and R. C. Cammarata, Editors, p. 596, IOP, Bristol, U.K. (1996).
- Handbook of Nanostructured Materials and Nanotechnology*, Vol. 1, Synthesis and Processing, H. S. Nalwa, Editor, p. 645, Elsevier, New York (2000).
- B. Wu, A. Heidelberg, and J. J. Boland, *Nat. Mater.*, **4**, 525 (2005).
- A. L. Santos, D. Profeti, and P. Olivi, *Electrochim. Acta*, **50**, 2615 (2005).
- L. Jiang, G. Sun, Z. Zhou, S. Sun, Q. Wang, S. Yan, H. Li, J. Tian, J. Guo, B. Zhou, and Q. Xin, *J. Phys. Chem. B*, **109**, 8774 (2005).
- F. G. Fagan and V. R. W. Amaral, *Am. Ceram. Soc. Bull.*, **72**, 119 (1993).
- S. A. Pianaro, P. R. Bueno, E. Longo, and J. A. Varela, *J. Mater. Sci. Lett.*, **14**, 692 (1995).
- J. Chen, M. Wang, B. Liu, Z. Fan, K. Cui, and Y. Kuang, *J. Phys. Chem. B*, **110**, 11775 (2006).
- P. H. Mutin, V. Lafond, A. F. Popa, G. M. L. Markey, and A. Dereux, *Chem. Mater.*, **16**, 5670 (2004).
- L. Xu, F. L. Li, and S. J. Dong, *J. Electroanal. Chem.*, **383**, 133 (1995).
- N. Y. Jia, R. B. Martin, Z. G. Qi, M. C. Lefebvre, and P. G. Pickup, *Electrochim. Acta*, **46**, 2863 (2001).
- S. L. Gojković, S. K. Zec, S. Savinell, *J. Electrochem. Soc.*, **145**, 3713 (1998).
- A. J. Bard and L. R. Faulkner, *Electrochemical Methods, Fundamentals and Applications*, Wiley, New York (1980).
- R. Woods, *J. Electroanal. Chem. Interfacial Electrochem.*, **9**, 1 (1976).
- T. Okanishi, T. Matsui, T. Takeguchi, R. Kikuchi, and K. Eguchi, *Appl. Catal., A*, **298**, 181 (2006).
- W. X. Chen, J. Y. Lee, and Z. Liu, *Chem. Commun. (Cambridge)*, **2002**, 2588.
- S. Litster and G. McLean, *J. Power Sources*, **130**, 61 (2004).